

# Beyond the Standard Model of Physics with Astronomical Observations

Research Article

Raul Jimenez<sup>1,2\*</sup>

1 ICREA & ICC, University of Barcelona (IEEC-UB), Marti i Franques 1, Barcelona 08028, Spain

2 Theory Group, Physics Department, CERN, CH-1211, Geneva 23, Switzerland

**Abstract:** There has been significant recent progress in observational cosmology. This, in turn, has provided an unprecedented picture of the early universe and its evolution. In this review I will present a (biased) view of how one can use these observational results to constraint fundamental physics and in particular physics beyond the standard model.

**Keywords:** Cosmology • Astronomy • Beyond the Standard Model

© Versita sp. z o.o.

## 1. Introduction

Over the last two decades we have seen phenomenal progress in our observational understanding of the Universe. It was in the early 90s that the first image of the fluctuation of the Cosmic Microwave Background (CMB) was obtained by the COBE satellite. It was around the same time that the first survey of galaxies was carried out by the CfA. Twenty years later we have had our knowledge of the cosmos revolutionised by the outstanding data collected by two galaxy surveys: 2dF and SDSS and by two CMB satellites WMAP & Planck, which have provided both full sky temperature and polarization measurements of the CMB. In fact, Planck has already obtained all information in the temperature power spectrum that is available in the scale (cosmic variance limited) at angular scales larger than  $5'$ . While these datasets have had a profound impact on our understanding of the cosmos, they also provide an invaluable tool to extract information about fundamental physics. The future is even brighter, because there are current and future cosmological experiments planned to map out the whole sky at all wavelengths. Further, the promise of detecting gravitational waves should be realised during this decade with advanced ground-based observatories like LIGO, and therefore a new window will open at mapping the Universe. In this talk, I will give a (presenter biased) view of some insights into fundamental physics that have been obtained using cosmological

\* *E-mail:* raul.jimenez@icc.ub.edu

observations. Namely: constraints on dark energy, neutrino masses and hierarchy and beyond the standard model physics. Most of the material shown here has been presented elsewhere in many of my own referred publications, but is presented here coherently to give a panchromatic view of how to shed light on beyond the standard model physics with cosmology.

## 2. Dark energy

Direct supernova measurements of the deceleration parameter [1], as well as indirect measurements based upon a combination of results from the cosmic microwave background (CMB) [2], large-scale structure (LSS) [3, 4], and the Hubble constant [5] indicate that the expansion is accelerating. This suggests either that gravity on the largest scales is described by some theory other than general relativity and/or that the Universe is filled with some sort of negative-pressure “dark energy” that drives the accelerated expansion [6]; either way, it requires new physics beyond general relativity and the standard model of particle physics. These observations have garnered considerable theoretical attention as well as observational and experimental efforts to learn more about the new physics coming into play.

The simplest possibility is to extend Einstein’s equation with a cosmological constant, or equivalently, to hypothesize a fluid with an equation-of-state parameter  $w \equiv p/\rho = -1$  (with  $p$  and  $\rho$  the pressure and energy density, respectively). However, it may well be that the cosmological “constant” actually evolves with time, in which case  $w \neq -1$ , and there are a variety of theoretical reasons [7] to believe that this is the case. Precise measurement of  $w(z)$  (with, in general, a parameterized redshift dependence) or, equivalently, the cosmic expansion history, has thus become a central goal of physical cosmology [8, 10].

Among the techniques to determine the cosmic expansion history are supernova searches, baryon acoustic oscillations (BAO) [11, 12, 14, 15], weak lensing [17], and galaxy clusters [16]. These techniques all have different strengths, and they all also suffer from a different set of weaknesses. As argued in the ESO/ESA and Dark Energy

$z$	BC03 models					MaStro models				
	$H(z)$	$\sigma_{stat}$	$\sigma_{syst}$	$\sigma_{tot}$	% error	$H(z)$	$\sigma_{stat}$	$\sigma_{syst}$	$\sigma_{tot}$	% error
0.1791	75	3.8	0.5	4	5%	81	4.1	2.5	5	6%
0.1993	75	4.9	0.6	5	7%	81	5.2	2.6	6	7%
0.3519	83	13	4.8	14	17%	88	13.9	7.9	16	18%
0.5929	104	11.6	4.5	13	12%	110	12.3	7.5	15	13%
0.6797	92	6.4	4.3	8	9%	98	6.8	7.1	10	11%
0.7812	105	9.4	6.1	12	12%	88	8	7.4	11	13%
0.8754	125	15.3	6	17	13%	124	14.3	8.7	17	14%
1.037	154	13.6	14.9	20	13%	113	10.1	11.7	15	14%

Table 1.  $H(z)$  measurements (in units of  $[\text{km s}^{-1}\text{Mpc}^{-1}]$ ) and their errors; the columns in the middle report the relative contribution of statistical and systematic errors, and the last ones the total error (estimated by summing in quadrature  $\sigma_{stat}$  and  $\sigma_{syst}$ ). These values have been estimated respectively with BC03 and MaStro stellar population synthesis models. This dataset can be downloaded at the address [http://www.astronomia.unibo.it/Astronomia/Ricerca/Progetti+e+attivita/cosmic\\_chronometers.htm](http://www.astronomia.unibo.it/Astronomia/Ricerca/Progetti+e+attivita/cosmic_chronometers.htm) (alternatively <http://start.at/cosmicchronometers>).

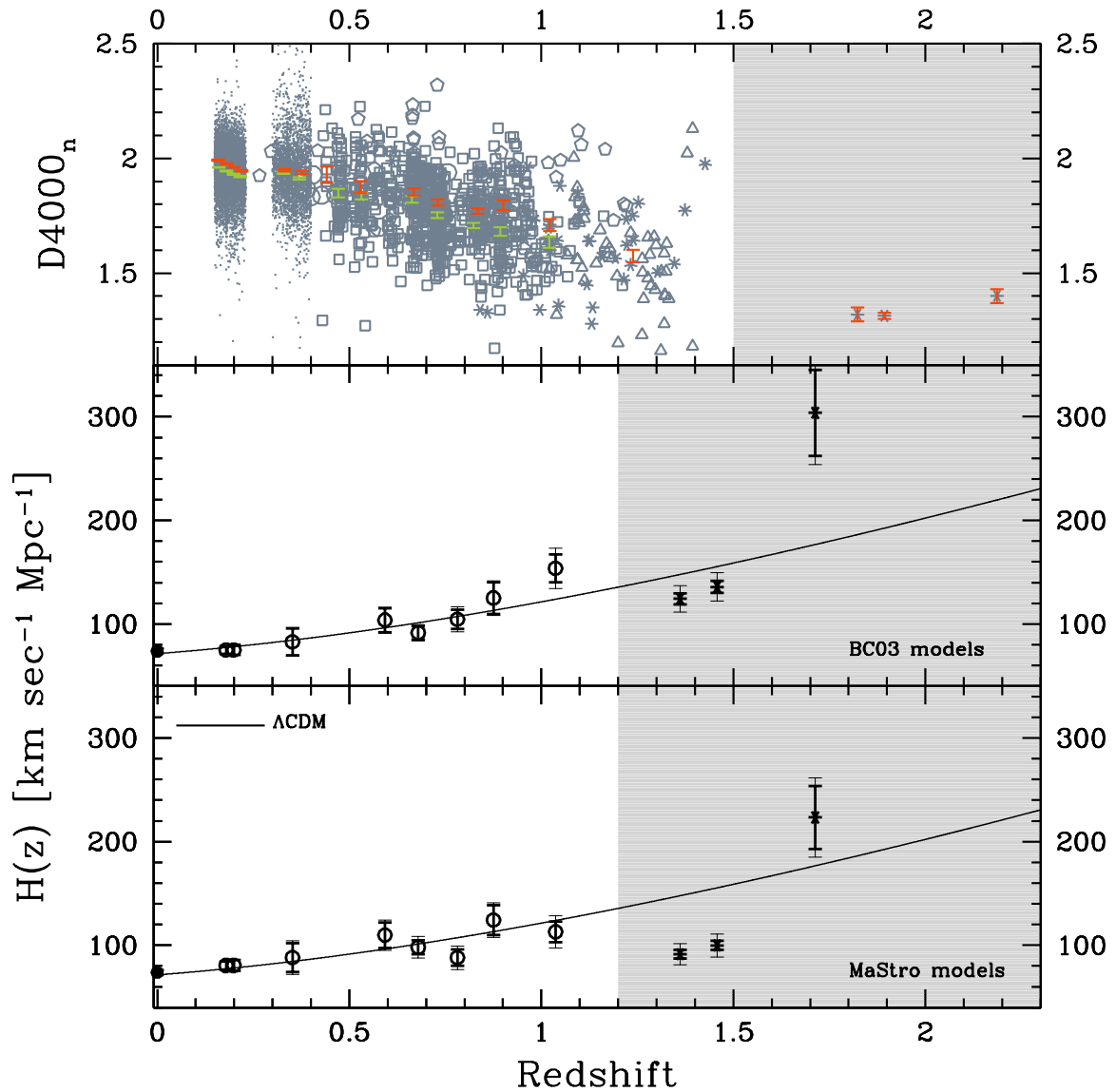
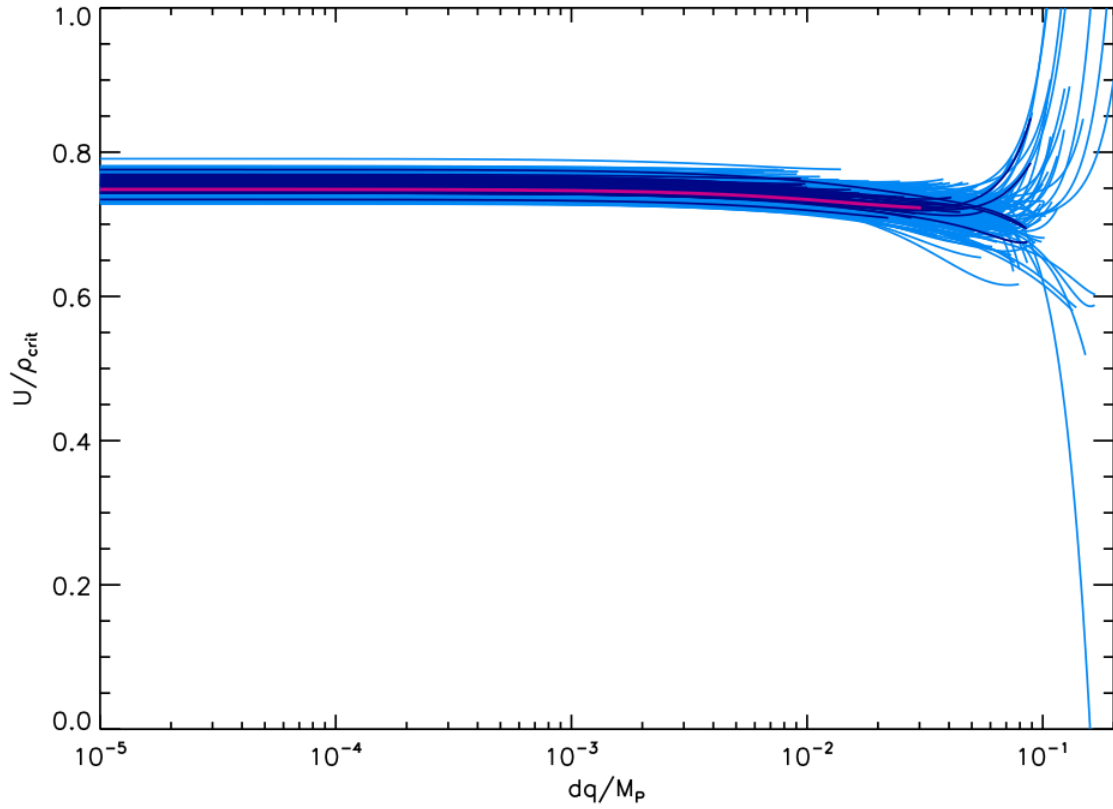


Figure 1. The  $H(z)$  measurement from a sample of passively evolving galaxies. The points at  $z > 1$  are taken from Ref. [33], while the point at  $z = 0$  is from the Hubble Key Project [5]. The solid line is the  $\Lambda$ CDM model.

Task Force reports [8, 10], robust conclusions about the cosmic expansion history will likely require several avenues to allow for cross checks. There may also still be room for other ideas for determining the expansion history.

A common weakness of supernova searches, BAO (at least the angular clustering), weak lensing, and cluster-based measurements is that they rely largely on integrated quantities. For example supernovae probe the luminosity distance,

$$d_L(z) = (1+z) \int_z^0 (1+z') \frac{dt}{dz'} dz'. \quad (1)$$



**Figure II.** The effective potential of accelerated expansion  $U(q)$  in units of the critical density  $\rho_{\text{crit}}$  as function of the displacement of the field  $q$  in  $M_{\text{p}}$  units. Different tracks are plotted for values with 68% confidence (dark blue lines) and 95% confidence (light blue lines). The best-fit model is shown as a solid red line, which is better described physically as a pseudo-Goldstone boson. The trajectories correspond to how much the field has moved in the full redshift range of the observational data ( $0 < z < 1.1$ ). Note that the potential is very flat at the few 6% level and that for many models the field displacement is very small. The data strongly favor a flat potential.

The other probes rely on similar quantities, which depend on an integral of the expansion history, to determine the expansion history, rather than the expansion history itself. The purpose of the differential-age technique [18] is to circumvent this limitation by measuring directly the integrand,  $dt/dz$ , or in other words, the change in the age of the Universe as a function of redshift. This can be achieved by measuring ages of galaxies with respect to a fiducial model, thus circumventing the need to compute absolute ages. From Galactic globular clusters age-dating we know that relative ages are much more accurately determined than absolute ages (e.g., Refs. [19–21]). A preliminary analysis, with archival data, has already been carried out [22, 23], and the results applied to constrain dark-energy theories (e.g., Refs. [24]).

The challenge with the differential-age measurement is to find a population of standard clocks and accurately date them. There is now growing observational evidence that the most massive galaxies contain the oldest stellar populations up to redshifts of  $z \sim 1 - 2$  [25–29]. Refs. [28] and [30] have shown that the most massive galaxies have less than 1% of their present stellar mass formed at  $z < 1$ . Ref. [29] shows that star formation in massive

systems in high-density regions — i.e., galaxy clusters — ceased by redshift  $z \sim 3$  and Ref. [31] shows that massive systems, those with stellar masses  $> 5 \times 10^{11} M_{\odot}$ , have finished their star-formation activity by  $z \sim 2$ . There is thus considerable empirical evidence for a population of galaxies, harboured in the highest-density regions of galaxy clusters, that has formed its stellar population at high redshift,  $z > 2$ , and that since that time this population has been evolving passively, without further episodes of star formation. These galaxies trace the “red envelope,” and are the oldest objects in the Universe at every redshift. The differential ages of these galaxies should thus be a good indicator for the rate of change of the age of the Universe as a function of redshift.

The most recent measurements of the expansion history obtained from the ages of passively-evolving galaxies in galaxy clusters at  $z < 2.0$  have been reported by [32–34] (see Fig. 1 and Table 1). Such observations provide a promising new cosmological constraint, particularly for understanding the evolution of the dark-energy density (Fig. II). The current measurements already provide valuable constraints [35–37], and the success of this effort should motivate further measurements along these lines as well as a more intensive investigation of the theoretical underpinnings of the calculations and the associated uncertainties. Further, there has been significant advancement in the last few years in modelling stellar populations of LRG galaxies and the differential technique has been recently applied very successfully to determine the metallicity of LRGs.

*The main highlight is that the expansion history of the Universe is consistent with that predicted by a flat potential, i.e. a cosmological constant. The data do not require extra parameters beyond a constant term in the Lagrangian to explain the current accelerated expansion.* Further, deviations in the potential from a constant are constrained to be below 6%. Observational constraints allow the parameters describing the Lagrangian to vary only within certain limits; the relative range of the allowed variation of the parameters confirms a well defined hierarchy where the linear and quadratic terms dominate over higher-order terms, justifying the basic assumption of the effective theory approach. Observational constraints also give some indications of the relevant energy scales involved. Because a direct determination of a Lagrangian allows us to determine the underlying symmetries in the theory, our results can be used to shed light on this as well.

Additional effort on both the theoretical and observational side may ultimately promote the differential-age technique as an important new dark-energy avenue which complements supernova searches, weak lensing, baryon acoustic oscillations, and cluster abundances. The differential-age technique can potentially provide *model independent* measurements of the expansion history of the universe at the % level [38–41]. Also, absolute ages of stellar ages have proven very valuable to establish possible deviations from the  $\Lambda$ CDM model [42, 43]

### 3. Measuring the neutrino mass and its hierarchy

In the past decade, there has been great progress in neutrino physics. It has been shown that atmospheric neutrinos exhibit a large up-down asymmetry in the SuperKamiokande (SK) experiment. This was the first significant evidence for a finite neutrino mass [44] and hence the incompleteness of the Standard Model of particle physics.

Accelerator experiments [45, 46] have confirmed this evidence and improved the determination of the neutrino mass splitting required to explain the observations. The Sudbury Neutrino Observatory (SNO) experiment has shown that the solar neutrinos change their flavors from the electron type to other active types (muon and tau neutrinos)[47]. Finally, the KamLAND reactor anti-neutrino oscillation experiments reported a significant deficit in reactor anti-neutrino flux over approximately 180 km of propagation [48]. Combining results from the pioneering Homestake experiment [49] and Gallium-based experiments [50], the decades-long solar neutrino problem [51] has been solved by the electron neutrinos produced at Sun’s core propagating adiabatically to a heavier mass eigenstate due to the matter effect [52].

As a summary, two hierarchical neutrino mass splittings and two large mixing angles have been measured, while only a bound on a third mixing angle has been established. Furthermore the standard model has three neutrinos and the motivation for considering deviations from the standard model in the form of extra neutrino species has now disappeared [54, 55].

New neutrino experiments aim to determine the remaining parameters of the neutrino mass matrix and the nature of the neutrino mass. Meanwhile, relic neutrinos produced in the early universe are hardly detectable by weak interactions but new cosmological probes offer the opportunity to detect relic neutrinos and determine neutrino mass parameters.

It is very relevant that the maximal mixing of the solar mixing angle is excluded at a high significance. The exclusion of the maximal mixing by SNO [47] has an important impact on a deep question in neutrino physics: “are neutrinos their own anti-particle?”. If the answer is yes, then neutrinos are Majorana fermions; if not, they are Dirac. If neutrinos and anti-neutrinos are identical, there could have been a process in the Early Universe that affected the balance between particles and anti-particles, leading to the matter anti-matter asymmetry we need to exist [56]. This question can, in principle, be resolved if neutrinoless double beta decay is observed. Because such a phenomenon will violate the lepton number by two units, it cannot be caused if the neutrino is different from the anti-neutrino (see [53] and references therein). Many experimental proposals exist that will increase the sensitivity to such a phenomenon dramatically over the next ten years (e.g., [57] and references therein).

The crucial question cosmology can address is if a negative result from such experiments can lead to a definitive statement about the nature of neutrinos. Within three generations of neutrinos, and given all neutrino oscillation data, there are three possible mass spectra: a) degenerate, with mass splitting smaller than the neutrino masses, and two non-degenerate cases, b) normal hierarchy, with the larger mass splitting between the two more massive neutrinos and c) inverted hierarchy, with the smaller spitting between the two higher mass neutrinos. For the inverted hierarchy, a lower bound can be derived on the effective neutrino mass [53]. The bound for the degenerate spectrum is stronger than for inverted hierarchy. Unfortunately, for the normal hierarchy, one cannot obtain a similar rigorous lower limit.

Neutrino oscillation data have measured the neutrino squared mass differences, which are hierarchical. Given the smallness of neutrino masses and the hierarchy in mass splittings, we can characterize the impact of neutrino

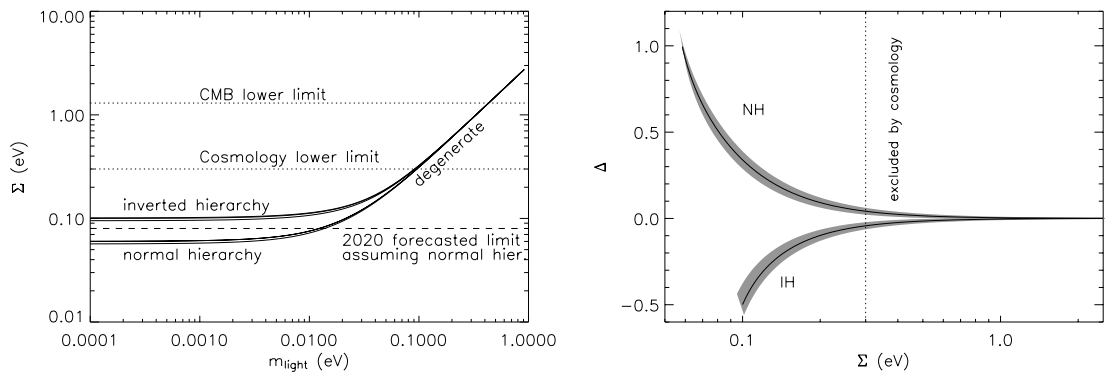


**Figure III.** Left: constraints from neutrino oscillations and from cosmology in the  $m$ - $\Sigma$  plane. Right: constraints from neutrino oscillations (shaded regions) and from cosmology in the  $\Sigma$ - $\Delta$  plane. In this parameterization the sign of  $\Delta$  specifies the hierarchy.

masses on cosmological observables and in particular on the the matter power spectrum by two parameters: the total mass  $\Sigma$  and the ratio of the largest mass splitting to the total mass,  $\Delta$ . One can safely neglect the impact of the solar mass splitting in cosmology. In this approach, two masses characterize the neutrino mass spectrum, the lightest one,  $m$ , and the heaviest one,  $M$ .

Neutrino oscillation data are unable to resolve whether the mass spectrum consists in two light states with mass  $m$  and a heavy one with mass  $M$ , named normal hierarchy (NH) or two heavy states with mass  $M$  and a light one with mass  $m$ , named inverted hierarchy (IH). Near future neutrino oscillation data may resolve the neutrino mass hierarchy if one of the still unknown parameters that relates flavor with mass states is not too small. On the contrary, if that mixing angle is too small, oscillation data may be unable to solve this issue. Analogously, a total neutrino mass determination from cosmology will be able to determine the hierarchy only if the underlying model is normal hierarchy and  $\Sigma < 0.1$  eV (see e.g., Fig III). If neutrinos exist in either an inverted hierarchy or are degenerate, (and if the neutrinoless double beta decay signal is not seen within the bounds determined by neutrino oscillation data), then the three light neutrino mass eigenstates (only) will be found to be Dirac particles. Massive neutrinos affect cosmological observations in a variety of different ways. For example, cosmic microwave background (CMB) data alone constrain the total neutrino mass  $\Sigma < 1.3$  eV at the 95% confidence level [58]. Neutrinos with mass  $< 1\text{eV}$  become non-relativistic after the epoch of recombination probed by the CMB, thus massive neutrinos alter matter-radiation equality for a fixed  $\Omega_m h^2$ . After neutrinos become non-relativistic, their free streaming damps the small-scale power and modifies the shape of the matter power spectrum below the free-streaming length. Combining large-scale structure and CMB data, at present the sum of masses is constrained to be  $\Sigma < 0.3$  eV [59]. Forthcoming large-scale structure data promise to determine the small-scale ( $0.1 < k < 1$  h/Mpc) matter power spectrum exquisitely well and to yield errors on  $\Sigma$  well below 0.1 eV (e.g., [60–62]).

The effect of neutrino mass on the CMB is related to the physical density of neutrinos, and therefore the mass difference between eigenstates can be neglected. However individual neutrino masses can have an effect on the large-scale shape of the matter power spectrum. In fact, neutrinos of different masses have different transition redshifts from relativistic to non-relativistic behavior, and their individual masses and their mass splitting change the details of the radiation-domination to matter-domination regime. As a result the detailed shape of the matter power spectrum on scales  $k \sim 0.01 h/\text{Mpc}$  is affected. In principle therefore a precise measurement of the matter power spectrum shape can give information on both the sum of the masses and individual masses (and thus the hierarchy), even if the second effect is much smaller than the first.

We define the relation between the neutrino masses  $m$  and  $M$  and the parameters  $\Sigma$  and  $\Delta$  as

$$\text{NH:} \quad \Sigma = 2m + M \quad \Delta = (M - m)/\Sigma \quad (2)$$

$$\text{IH:} \quad \Sigma = m + 2M \quad \Delta = (m - M)/\Sigma \quad (3)$$

(recall that  $m$  denotes the lightest neutrino mass and  $M$  the heaviest).

In Fig III we show the current constraints on neutrino mass properties in the  $m$ - $\Delta$  and  $\Sigma$ - $\Delta$  planes. While many different parameterizations have been proposed in the literature to account for neutrino mass splitting in a cosmological context [63, 65, 66] here we advocate using the  $\Delta$  parameterization for the following reasons.  $\Delta$  changes continuously through normal, degenerate and inverted hierarchies;  $\Delta$  is positive for NH and negative for IH. Finally, see Ref.[64], cosmological data are sensitive to  $\Delta$  in an easily understood way through the largest mass splitting (i.e., the absolute value of  $\Delta$ ), while the direction of the splitting (the sign of  $\Delta$ ) introduces a sub-dominant correction to the main effect. This parameterisation is strictly only applicable for  $\Sigma > 0$ , but oscillations experiments already set  $\Sigma > M > 0.05\text{eV}$ .

It is important to note that not the entire parameter space in the  $\Sigma$ - $\Delta$  plane (or of any other parameterization of the hierarchy used in the literature) is allowed by particle physics constraints and should be explored: only the regions around the normal and inverted hierarchies allowed by neutrino oscillation experiments should be considered (see Fig III).

To gain a physical intuition on the effect of neutrino properties on cosmological observables, such as the shape of the matter power spectrum, it is useful to adopt the following analytical approximation, as described in Ref. [65]. The matter power spectrum can be written as:

$$\frac{k^3 P(k; z)}{2\pi^2} = \Delta_R^2 \frac{2k^2}{5H_0^2 \Omega_m^2} D_\nu^2(k, z) T^2(k) \left( \frac{k}{k_0} \right)^{(n_s-1)}, \quad (4)$$

where  $\Delta_R^2$  is the primordial amplitude of the fluctuations,  $n_s$  is the primordial power spectrum spectral slope,  $T(k)$  denotes the matter transfer function and  $D_\nu(k, z)$  is the scale-dependent linear growth function, which encloses the dependence of  $P(k)$  on non-relativistic neutrino species.



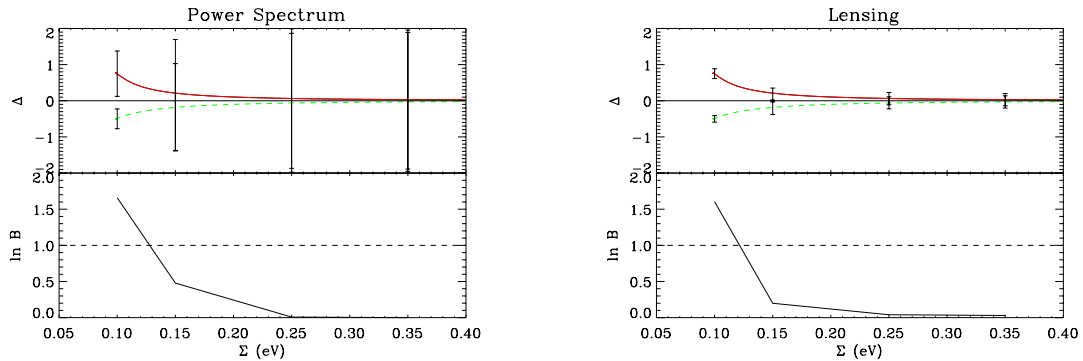


**Figure IV.** LSS (left) and Weak Lensing (right) forecasts for neutrino mass parameters  $\Sigma$  and  $\Delta$ . We assume the LSS survey consists of a comoving volume of  $600 \text{ Gpc}^3$  at  $z = 2$  and  $2000 \text{ Gpc}^3$  at  $z = 5$ . The Weak Lensing survey covers  $40,000 \text{ sq. deg.}$  with a median redshift of  $3.0$  and a number density of  $150$  galaxies per square arcminute. Several fiducial models ( $\Sigma, \Delta$ ) were used to derive by Fisher matrix approach the expected errors. The upper panel shows the  $1\text{-}\sigma$  errors on  $\Delta$  and  $\Sigma$ , the errors in  $\Sigma$  are so small that are barely visible. The lower panel shows the expected evidence ratio between the normal and inverted constraints as a function of neutrino mass. The dashed line shows the  $\ln B = 1$  level: in Jeffrey's scale  $\ln B < 1$  is 'inconclusive' evidence, and  $1 < \ln B < 2.5$  corresponds to 'substantial' evidence.

Each of the three neutrinos contributes to the neutrino mass fraction  $f_{\nu,i}$  where  $i$  runs from 1 to 3,

$$f_{\nu,i} = \frac{\Omega_{\nu,i}}{\Omega_m} = 0.05 \left( \frac{m_{\nu_i}}{0.658 \text{ eV}} \right) \left( \frac{0.14}{\Omega_m h^2} \right) \quad (5)$$

and has a free-streaming scale  $k_{\text{fs},i}$ ,

$$k_{\text{fs},i} = 0.113 \left( \frac{m_{\nu_i}}{1 \text{ eV}} \right)^{1/2} \left( \frac{\Omega_m h^2}{0.14} \frac{5}{1+z} \right)^{1/2} \text{ Mpc}^{-1}. \quad (6)$$

Analogously, one can define the corresponding quantities for the combined effect of all species, by using  $\Sigma$  instead of  $m_{\nu_i}$ . Since we will only distinguish between a light and a heavy eigenstate we will have e.g.,  $f_{\nu,m}, f_{\nu,\Sigma}, k_{\text{fs},m}, k_{\text{fs},\Sigma}$  etc., where in the expression for  $f_{\nu,m}$  one should use the mass of the eigenstate (which is the mass of the individual neutrino, or twice as much depending on the hierarchy) while in  $k_{\text{fs},m}$  one should use the mass of the individual neutrino.

The dependence of  $P(k)$  on non-relativistic neutrino species is in  $D_\nu(k, z)$ , given by

$$D_{\nu_i}(k, z) \propto (1 - f_{\nu_i}) D(z)^{1-p_i} \quad (7)$$

where  $k \gg k_{\text{fs},i}(z)$  and  $p_i = (5 - \sqrt{25 - 24f_{\nu_i}})/4$ . The standard linear growth function  $D(z)$  fitting formula is taken from [67].

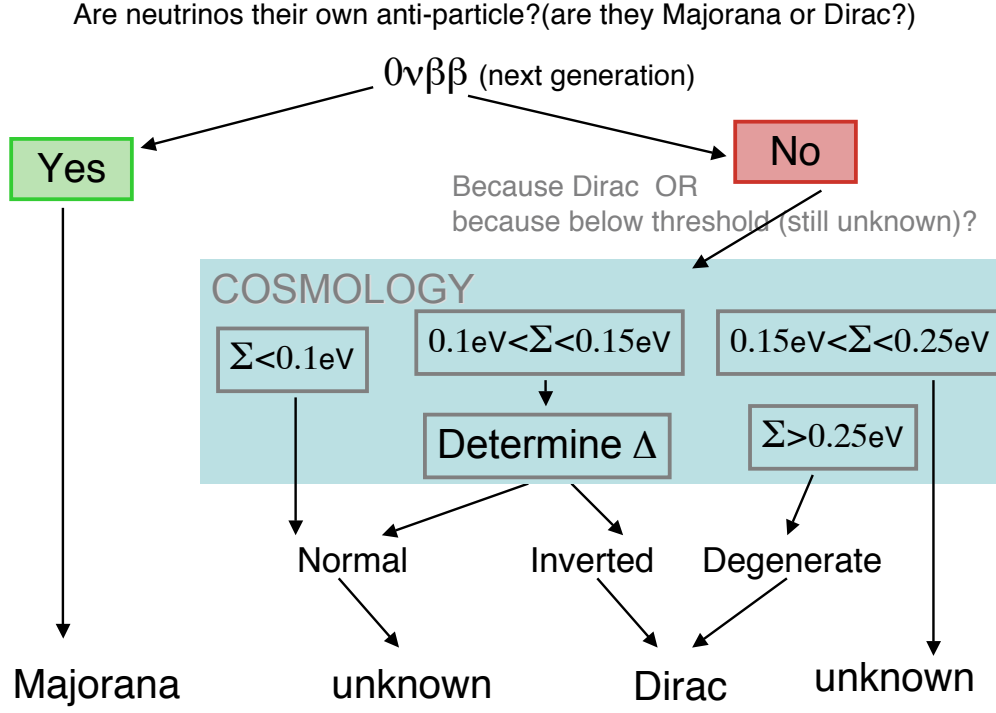


**Figure V.** Role of cosmology in determining the nature of neutrino mass. Future neutrinoless double beta decay ( $0\nu\beta\beta$ ) experiments and future cosmological surveys will be highly complementary in addressing the question of whether neutrinos are Dirac or Majorana particles. Next generation means near future experiments whose goal is to reach a sensitivity to the neutrinoless double beta decay effective mass of 0.01 eV. We can still find two small windows where this combination of experiments will not be able to give a definite answer, but this region is much reduced by combining  $0\nu\beta\beta$  and cosmological observations.

In summary there are three qualitatively different regimes in  $k$ -space that are introduced by the neutrino mass splitting

$$D_\nu(k, z) = D(k, z) \quad k < k_{fs,m} \quad (8)$$

$$D_\nu(k, z) = (1 - f_{\nu,m})D(z)^{(1-p_m)} \quad k_{fs,m} < k < k_{fs,\Sigma} \quad (9)$$

$$D_\nu(k, z) = (1 - f_{\nu,\Sigma})D(z)^{(1-p_\Sigma)} \quad k > k_{fs,\Sigma}, \quad (10)$$

where the subscript  $m$  refers to the light neutrino eigenstate and  $\Sigma$  to the sum of all masses.

This description is, however, incomplete: the transitions between the three regimes is done sharply in  $k$  while in reality the change is very smooth. In addition, the individual masses change the details of the matter-radiation transition which (keeping all other parameters fixed) adds an additional effect at scales  $k > k_{fs,\Sigma}$ .

In order to explore what constraints can be placed on  $\Delta$  and  $\Sigma$  for a given survey set-up we can use a Fisher

matrix approach. The elements of  $\mathbf{F}$ , the Fisher information matrix [68], are given by

$$F_{\theta\gamma} = -2 \left\langle \frac{\partial^2 \ln L}{\partial \theta \partial \gamma} \right\rangle \quad (11)$$

where  $\theta$  and  $\gamma$  denote cosmological parameters (and the Fisher matrix element's indices) and  $L$  denotes the likelihood of the data given the model. Marginalised errors on a parameter are computed as  $\sigma^2(\theta) = (\mathbf{F}^{-1})_{\theta\theta}$ . We can also calculate expected Bayesian evidence for cosmological parameters using the approach of Ref. [69, 70]. In the case that we are considering we use the formula from [70] for the expectation value of the evidence, in this case the expected Bayes factor is simply the log of ratio of the Fisher determinants.

Following Ref. [71] the Fisher matrix for the galaxy power spectrum is

$$F_{\theta\gamma} = \frac{V_s}{8\pi^2} \int_{-1}^1 d\mu \int_{k_{\min}}^{k_{\max}} k^2 dk N \frac{\partial \ln P(k, \mu)}{\partial \theta} \frac{\partial \ln P(k, \mu)}{\partial \gamma} \quad (12)$$

with  $N = [nP(k, \mu)/(nP(k, \mu) + 1)]^2$  and  $V_s$  is the volume of the survey. The integration over the projected angle along the light of sight <sup>1</sup>  $\mu$  is analytical and the maximum and minimum wavenumbers allowed depend on the survey characteristics with the constraint that  $k_{\max}$  must be in the linear regime. The derivatives are computed at the fiducial model chosen.

The degeneracies between  $\Sigma$  and  $\Delta$  are small, and the very small constraint on  $\Sigma$  results in the constraints being effectively un-correlated in the  $\Sigma$ - $\Delta$  plane. We note that the constraints on  $\Delta$  around the IH and NH peaks are tighter for weak lensing than LSS, this is due to lensing providing constraints on both the geometry and the growth of structure, which provides a smaller raw constraint and a more orthogonal constraint to the CMB resulting in smaller errors. Interestingly, even though the weak lensing constraints on  $\Delta$  are smaller than for the power spectrum, the evidence ratio is comparable (see Fig. IV), because, due to the multi-dimensional degeneracy directions, a naive correspondence between error-bars and evidence is not applicable (it is to a first approximation the difference between the two error bars that is important).

Note that the evidence calculation explicitly assumes two isolated peaks, and so is only applicable when the fiducial points are separated by multiple-sigma. As a result of this, the evidence calculations may be slightly optimistic for large masses. However, for  $\Sigma < 0.2$  eV, the  $\chi^2$  difference between the two minima becomes noticeable as well as the shift between the location of one of the two minima and the central  $\Delta$  value for the oscillations experiments (which induces an additional  $\chi^2$  difference). While this information is not fully accounted for in a Bayesian approach to forecasting the evidence, it may be included at the moment of analyzing the data, using different approaches such as the likelihood ratio, and may slightly improve the significance for the hierarchy determination. While we have used the oscillation results to center the Fisher and evidence calculations on the NH and IH, combining the oscillation experiments constraints will not improve the evidence; in fact, oscillation experiments

<sup>1</sup> As it is customary,  $\mu$  denotes the cosine of the angle with respect to the line of sight.

give symmetric errors on  $\Delta$  (i.e. they do not depend on the sign of  $\Delta$ ). The final scheme is shown in Fig. V which illustrates how the hierarchy can be determined in future cosmology experiments.

Better perspectives at measuring the neutrino hierarchy from the sky can be attained by exploiting the non-linear part of the power spectrum of galaxies as was shown by Ref. [72]. Non-linearities enhance the dependence of the power spectrum on the different neutrino hierarchies, thus making the observational signature more pronounced. If all other cosmological parameters are known (including the sum of neutrino masses  $\Sigma$ ), the two hierarchies can be distinguished with confidence, as illustrated in Fig. VII as function of the maximum  $k$  considered, making the effect potentially measurable. We have assumed an effective volume of  $1(\text{Gpc}/h)^3$  at  $z = 0$  (red lines) and  $10(\text{Gpc}/h)^3$  at  $z = 1$  (blue lines).<sup>2</sup> Whether degeneracies with other cosmological parameters and systematic effects (galaxy bias, baryonic physics, observational limitations etc.) will cancel the detectability of the effect remains to be explored.

Cosmology has the potential of determining the neutrino hierarchy in the interesting window  $\Sigma \gtrsim 0.1\text{eV}$ . Signal-to-noise estimates done using linear theory predictions indicated that if  $\Sigma$  happens to be in the window  $0.15\text{eV} < \Sigma < 0.25\text{eV}$ , cosmology could not help determine the hierarchy and thus the nature of neutrino masses [64], leaving an important gap in our knowledge of neutrino properties. The fact that non-linearities enhance the effect compared to the linear prediction, will potentially enable cosmology to determine the hierarchy in a wider  $\Sigma$  range and possibly close the gap.

As an aside and already noted in Ref. [64], cosmology is more sensitive to  $|\Delta|$  than to its sign: a measurement of  $|\Delta|$  in agreement with that predicted by oscillations experiments for the measured  $\Sigma$  would provide a convincing consistency check for the total neutrino mass constraint from cosmology.

## 4. Using astronomical distances to constraint beyond the standard model physics

Cosmological observations provide constraints on different distance measures: luminosity distance (as provided e.g., by supernovae), angular diameter distance (as provided e.g., by baryon acoustic oscillations) and even on the expansion rate or the Hubble parameter as a function of redshift  $z$ . Both luminosity distance and angular diameter distance are functions of the Hubble parameter. While combining these measurements helps to break parameter degeneracies and constrain cosmological parameters, comparing them helps to constrain possible deviations from the assumptions underlying the standard cosmological model (e.g. isotropy), or to directly constrain physics beyond the standard model of particle physics (e.g. couplings of photons to scalar or pseudo-scalar matter).

The Etherington relation [73] implies that, in a cosmology based on a metric theory of gravity, distance measures

---

<sup>2</sup> *These volumes roughly correspond to the volume out to  $z = 0.5$  and between  $z = 0.5$  and  $z = 1.5$  in 1/10 of the sky respectively in a standard  $\Lambda\text{CDM}$  universe.*

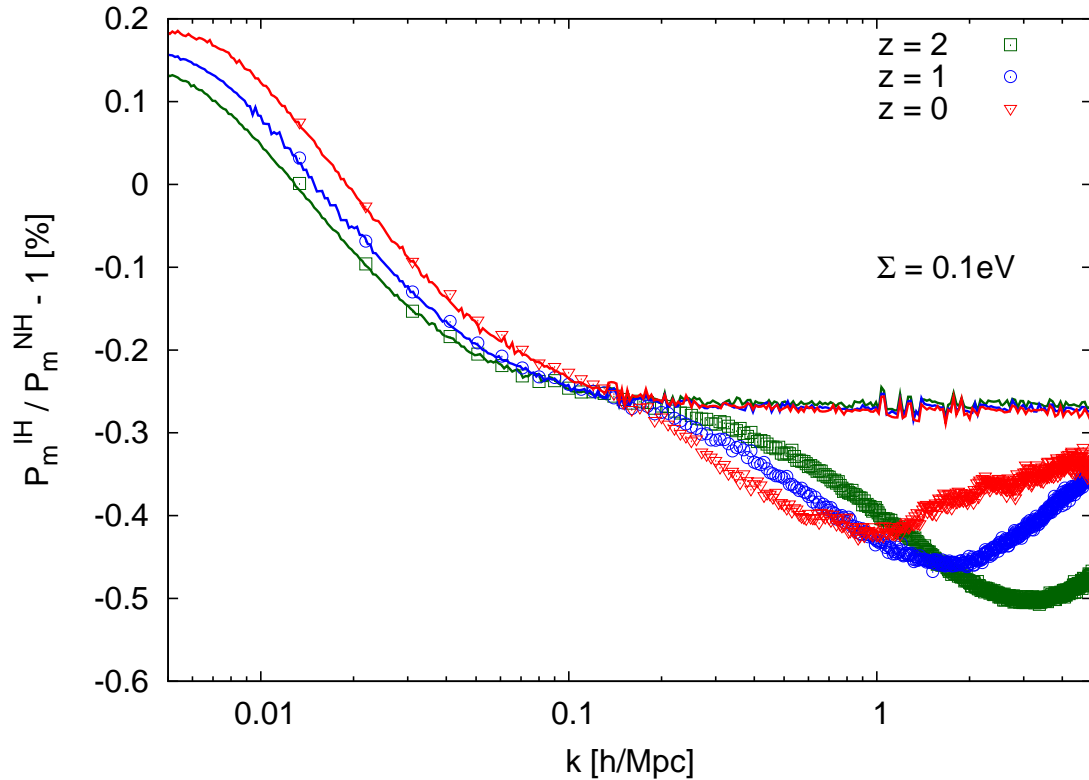


Figure VI. Fractional difference in the total matter power spectrum (CDM+baryons+massive neutrinos) of the inverted hierarchy and normal hierarchy run (the sum of neutrino masses is kept fixed and only the mass splitting is varied). Note that also in this case, non-linearities enhance the effect on mildly non-linear scales compared to linear theory predictions (solid lines).

are unique: the luminosity distance is  $(1+z)^2$  times the angular diameter distance. This is valid in any cosmological background where photons travel on null geodesics and where, crucially, photon number is conserved.

There are several scenarios in which the Etherington relation would be violated: for instance we can have deviations from a metric theory of gravity, photons not traveling along unique null geodesics, variations of fundamental constants, etc. Here we want to restrict our attention to violations of the Etherington relation arising from the violation of photon conservation.

A change in the photon flux during propagation towards the Earth will affect the Supernovae (SNe) luminosity distance measures but not the determinations of the angular diameter distance. Photon conservation can be violated by simple astrophysical effects or by exotic physics. Amongst the former we find, for instance, attenuation due to interstellar dust, gas and/or plasmas. Most known sources of attenuation are expected to be clustered and can be typically constrained down to the 0.1% level [74, 75]. Unclustered sources of attenuation are however much more difficult to constrain. For example, gray dust [76] has been invoked to explain the observed dimming of Type Ia Supernovae without resorting to cosmic acceleration.

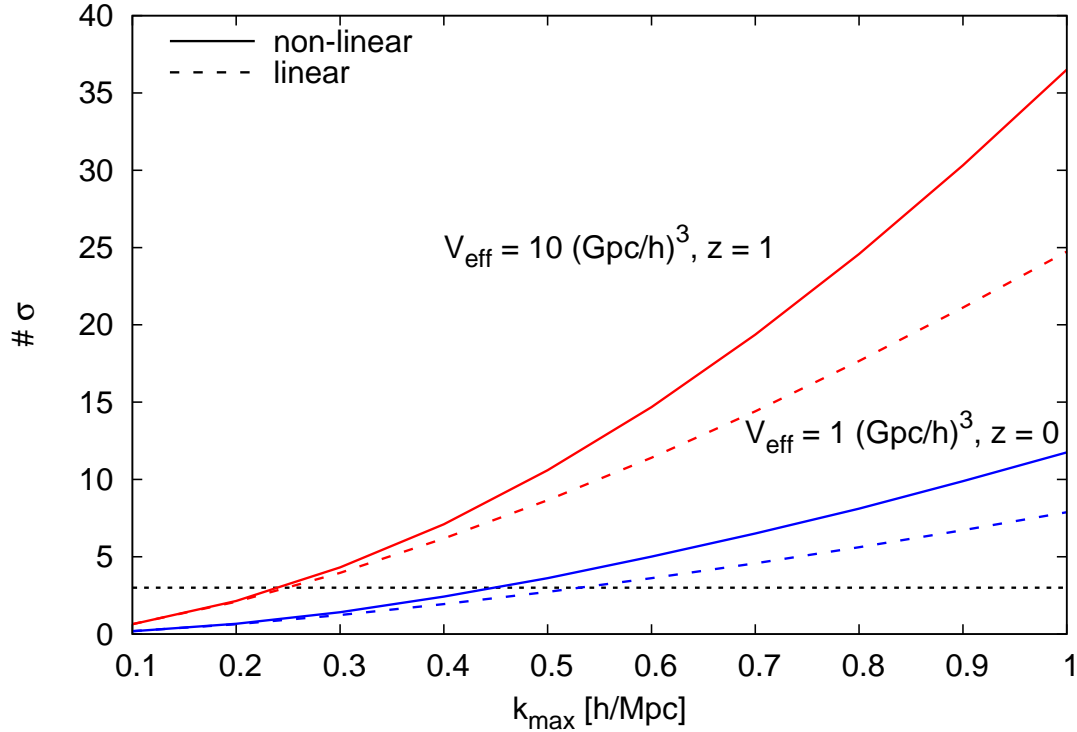


Figure VII. Forecast of the number of sigmas separating the two hierarchies for  $\Sigma = 0.1\text{eV}$  as a function of the maximum  $k$  vector considered and for two effective volumes  $1$  and  $10 (\text{Gpc}/h)^3$  at  $z = 0$  and  $z = 1$  respectively. It is assumed that all other cosmological parameters are known. The horizontal dotted line indicates the  $3 - \sigma$  level.

More exotic sources of photon conservation violation involve a coupling of photons to particles beyond the standard model of particle physics. Such couplings would mean that, while passing through the intergalactic medium, a photon could disappear –or even (re)appear!– interacting with such exotic particles, modifying the apparent luminosity of sources. Here we consider the mixing of photons with scalars, known as axion-like particles, and the possibility of mini-charged particles which have a tiny, and unquantised electric charge. A recent review [77] highlights the rich phenomenology of these weakly-interacting-sub-eV-particles (WISPs), whose effects have been searched for in a number of laboratory experiments and astronomical observations. In particular, the implications of this particles on the SN luminosity have been described in a number of publications [78–82].

One of the most interesting features of these models is that the exotic opacity involved could in principle “mimic” the value of a non-zero cosmological constant inferred from SNe measurements. However, this possibility can already be excluded (at least in the simplest WISP models) by the absence of distortions in the CMB or the spectra of quasars for axion-like-particles, and by arguments of stellar evolution in the case of mini-charged particles.

## 4.1. Calculating cosmic opacity

In reference [93], the authors use Type Ia SN brightness data (namely the SCP Union 2008 compilation [94]) in combination with measurements of cosmic expansion  $H(z)$  from differential aging of luminous red galaxies (LRGs) [23, 95] to obtain constraints on non-trivial opacity, at cosmological scales. The basic idea is to study possible violations from the ‘‘Etherington relation’’ [73], the distance duality between luminosity distance,  $d_L$ , and angular diameter distance,  $d_A$ :

$$d_L(z) = (1+z)^2 d_A(z). \quad (13)$$

This identity depends only on photon number conservation and local Lorentz invariance. It holds for general metric theories of gravity, where photons travel along unique null geodesics. Since Lorentz violation is strongly constrained for the low energies corresponding to optical observations [83], the study of possible violations of Eq. (13) through SN observations directly constrains photon number violation. Any such systematic violations can then be interpreted as an opacity effect in the observed luminosity distance, parametrised through a generic opacity parameter,  $\tau(z)$ , as:

$$d_{L,obs}^2 = d_{L,true}^2 e^{\tau(z)}. \quad (14)$$

Note that this ‘‘opacity’’ can have in principle both signs. In other words, this parametrisation also allows for apparent *brightening* of light sources, as would be the case, for example, if exotic particles were also emitted from the source and converted into photons along the line of sight [81]. From Eq. (14) it is clear that the inferred distance moduli for the observed SNe picks an extra term which is linear in  $\tau(z)$ :

$$DM_{obs}(z) = DM_{true}(z) + 2.5[\log e]\tau(z). \quad (15)$$

On the other hand, one can also use other determinations of distance measures, which are independent of  $\tau$ , to constrain possible deviations from Eq. (13). This approach was initiated in reference [92] (see also [84–87] for related earlier work) where the authors used measurements [88] of the baryon acoustic oscillation (BAO) scale at two redshifts, namely  $z = 0.20$  and  $z = 0.35$ , to obtain a parameterization-independent upper-bound for the difference in opacity between these two redshifts,  $\Delta\tau < 0.13$  at 95% confidence. In reference [93] this constraint was improved (and also extended over a wider redshift range, but for a general parameterised form for  $\tau$ ) by using, instead of measurements of the BAO scale at these two redshifts, measurements of cosmic expansion  $H(z)$  from differential aging of LRGs at redshifts  $z < 2$ . This method of distance determination relies on the detailed shapes of galaxy spectra but not on galaxy luminosities, so it is independent of  $\tau$ .

In particular, the authors introduced a parameter  $\epsilon$  to study deviations from the Etherington relation of the form:

$$d_L(z) = d_A(z)(1+z)^{2+\epsilon}, \quad (16)$$

and constrained this parameter to be  $\epsilon = -0.01_{-0.09}^{+0.08}$  at 95% confidence. Restricted to the redshift range  $0.2 < z < 0.35$ , where  $\tau(z) = 2\epsilon z + \mathcal{O}(\epsilon z^2)$ , this corresponds to  $\Delta\tau < 0.02$  at 95% confidence. Below, we will apply similar

constraints on different parametrisations of  $\tau$  which correspond to particular models of exotic matter-photon coupling, namely axion-like particles (ALPs), chameleons, and mini-charged particles (MCPs).

Before moving to these models, we briefly update the above constraint on  $\epsilon$  using the latest  $H(z)$  data [32], which include two extra data points at redshifts  $z = 0.48$  and  $z = 0.9$ , as well as the latest determination of  $H_0$  [89]. Even though the addition of these two extra data points alone significantly improves the constraints of reference [93], the effect of  $H_0$  is also quite significant, because it acts as an overall scale in the distance measures, which is marginalised over a Gaussian prior, and the measurement error in this determination is about half of that of the HST Key Project determination [90] used in [93].

Fig. VIII shows the updated constraints obtained using the above data in combination with the SCP Union 2008 Compilation [94] of type Ia Supernova data, compared to the previous constraints of reference [93]. On the left, the darker blue contours correspond to the (two-parameter) 68% and 95% joint confidence levels obtained from SN data alone, while lighter blue contours are the corresponding confidence levels for  $H(z)$  data. Solid-line transparent contours are for joint SN+ $H(z)$  data. For comparison we also show the previous  $H(z)$  and SN+ $H(z)$  contours in dotted and dashed lines respectively. On the right we show one-parameter (marginalized over all other parameters) constraints on  $\epsilon$ , again for the current analysis (solid line) and for that of reference [93] (dotted). For the reader familiar with Bayesian methods, this plot corresponds to the posterior

$$P(\epsilon|S, E) = \int_{\Omega_m} \int_{H_0} P(\Omega_m, H_0|E)P(\epsilon, \Omega_m, H_0|S) d\Omega_m dH_0, \quad (17)$$

where  $P(\Omega_m, H_0|E)$  and  $P(\epsilon, \Omega_m, H_0|S)$  are the posterior probabilities for the corresponding model parameters, given the  $H(z)$  (Expansion) and SN (Supernovae) data respectively. These are given by the likelihoods of the two data sets in the model parameters, assuming Gaussian errors and using flat priors on all three parameters. In particular, we have taken  $\epsilon \in [-0.5, 0.5]$ ,  $\Omega_m \in [0, 1]$  and  $H_0 \in [74.2 - 3 \times 3.6, 74.2 + 3 \times 3.6]$  (Riess et. al. [89]), all spaced uniformly over the relevant intervals, in a flat  $\Lambda$ CDM model. Similarly, the solid line transparent contours on the left plot of Fig. VIII correspond to taking only the integral over  $H_0$  in the right hand side of Eq. (17), yielding, therefore, the two-parameter posterior  $P(\epsilon, \Omega_m|S, E)$ .

As seen in Fig. VIII, the improvement in these constraints is significant. The new result on  $\epsilon$ , marginalised over all other parameters, is  $\epsilon = -0.04_{-0.07}^{+0.08}$  at 95% confidence, which for redshifts between 0.2 and 0.35 (currently probed by BAO data), corresponds to a transparency (i.e.,  $\tau \geq 0$ ) bound  $\Delta\tau < 0.012$ , a factor of two tighter than the result in reference [93]<sup>3</sup>. We now move on to study more general parametrisations of cosmic opacity, tailored for particular models of exotic matter coupled to photons.

<sup>3</sup> Note that the data slightly favour negative  $\epsilon$  (thus the much stronger constraint on a positive  $\Delta\tau$ ), but only at  $< 1\text{-}\sigma$  level.



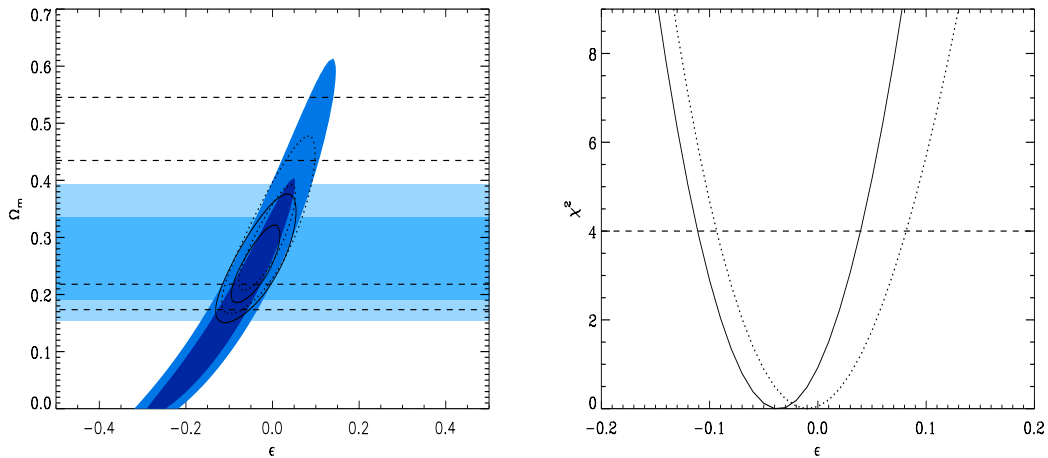


Figure VIII. Updated constraints of reference [93], using  $H(z)$  data [32] and the Riess et al. determination of  $H_0$  [89] in combination with the SCP Union 2008 SN Ia compilation. *Left*: Two-parameter constraints on the  $\epsilon - \Omega_m$  plane. Darker blue contours correspond to 68% and 95% confidence levels obtained from SN data alone, lighter blue contours are for  $H(z)$  data, and solid line transparent contours are for joint SN+ $H(z)$ . Previous  $H(z)$  and joint SN+ $H(z)$  from [93] are shown in dashed and dotted lines respectively. *Right*: One-parameter joint constraints on  $\epsilon$  for the current analysis (solid line) and that of reference [93] (dotted line). The dashed line shows the 95% confidence level,  $\Delta\chi^2 = 2$ .

## 4.2. Axion-like Particles and Chameleons

New scalar or pseudo scalar particles from physics beyond the standard model, here denoted as  $\phi$ , may couple to photons through

$$\mathcal{L}_{scalar} = \frac{1}{4M} F_{\mu\nu} F^{\mu\nu} \phi \quad (18)$$

and

$$\mathcal{L}_{pseudo-scalar} = \frac{1}{8M} \epsilon_{\mu\nu\lambda\rho} F^{\mu\nu} F^{\lambda\rho} \phi \quad (19)$$

where  $M$  is the energy scale of the coupling (another widely used notation is  $g_{\phi\gamma} = 1/M$ ),  $F_{\mu\nu}$  the electromagnetic field strength and  $\epsilon_{\mu\nu\lambda\rho}$  the Levi-Civita symbol in four dimensions. Such fields are collectively known as Axion-Like Particles (ALPs), as a coupling of the form (19) arises for the axion introduced by Peccei and Quinn (PQ) to solve the strong CP problem [96]. Interestingly, these fields also arise naturally in string theory (for a review see [97]).

Axions, or axion-like-particles, can arise from field theoretic extensions of the standard model as Goldstone bosons when a global shift symmetry, present in the high energy sector, is spontaneously broken. In the PQ axion case, this symmetry is colour anomalous and the explicit breaking makes the axion pick up a small mass. This mass is, up to a model-independent constant, proportional to the coupling (19). For a generic ALP, however, the mass is in principle independent of the strength of its coupling, and in particular can be zero if the related shift symmetry remains intact. That is, for instance, the case of Arions [98], the orthogonal combination of the PQ axion, if there are *two* independent colour anomalous shift symmetries.

Chameleon scalar fields are another very interesting type of ALPs [99]. They were originally invoked in [100, 101] to explain the current accelerated expansion of the Universe with a quintessence field which can couple to matter without giving rise to large fifth forces or unacceptable violations of the weak equivalence principle. The chameleon achieves this because its mass depends on the local energy density. The environmental dependence of the mass of the chameleon means that it avoids many of the constraints on the strength of the coupling, which normally apply to standard scalar and pseudo-scalar fields as they are derived from physics in dense environments. For a more detailed discussion see [102]. The cosmology of the chameleon was explored in detail in [103], the possibility of the chameleon coupling to photons was first discussed in [104] and such a coupling was shown to be generic in [99].

The Lagrangian terms given above mean that ALPs can affect the propagation of photons; in particular, if photons traverse a magnetic field there is a non-zero probability that they will oscillate into ALPs [105]. Notice however that only photons polarized perpendicular (parallel) to the magnetic field mix with scalar (pseudo-scalar) particles. Therefore, the interactions between photons and ALPs in the presence of a magnetic field not only imply that photon number is not conserved, but can also alter the polarization of the light beam. Both effects have been exploited in many searches for ALPs both in the laboratory and in astronomical observations, see [77] for a recent review.

If new particles from physics beyond the standard model couple to photons then the propagation of light may be altered. We have reviewed two scenarios for exotic particles which can significantly modify the propagation of photons as they pass through magnetic fields. Measurements of cosmic opacity are a strong tool to constrain such scenarios, as interactions between photons and exotic particles in the magnetic fields of the intergalactic medium leads to a new source of cosmic opacity. Uniform deviations from cosmic transparency (i.e. opacity) can be constrained through their effects on distance duality, by parameterizing possible deviations from the Etherington relation. The Etherington relation implies that, in a cosmology based on a metric theory of gravity, distance measures are unique: the luminosity distance is  $(1+z)^2$  times the angular diameter distance. Both luminosity distance and angular diameter distance depend on the Hubble parameter  $H(z)$ , but this relation is valid in any cosmological background where photons travel on null geodesics and where, crucially, photon number is conserved. We have restricted our attention on violations of the Etherington relation arising from the violation of photon conservation.

More exotic sources of photon-conservation violation involve a coupling of photons to particles beyond the standard model of particle physics. We have focused on axion-like particles, new scalar or pseudo scalar fields which couple to the kinetic terms of photons, and mini-charged particles which are hidden sector particles with a tiny electric charge. Photons passing through intergalactic magnetic fields may be lost by pair production of light mini-charged particles. If the mixing between axion-like particles and photons is significant, then interactions in the intergalactic magnetic fields will also lead to a loss of photons due to conversion into ALPs. However if the coupling between photons and ALPs is sufficiently strong, one-third of any initial flux will be converted into ALPs, and two-thirds

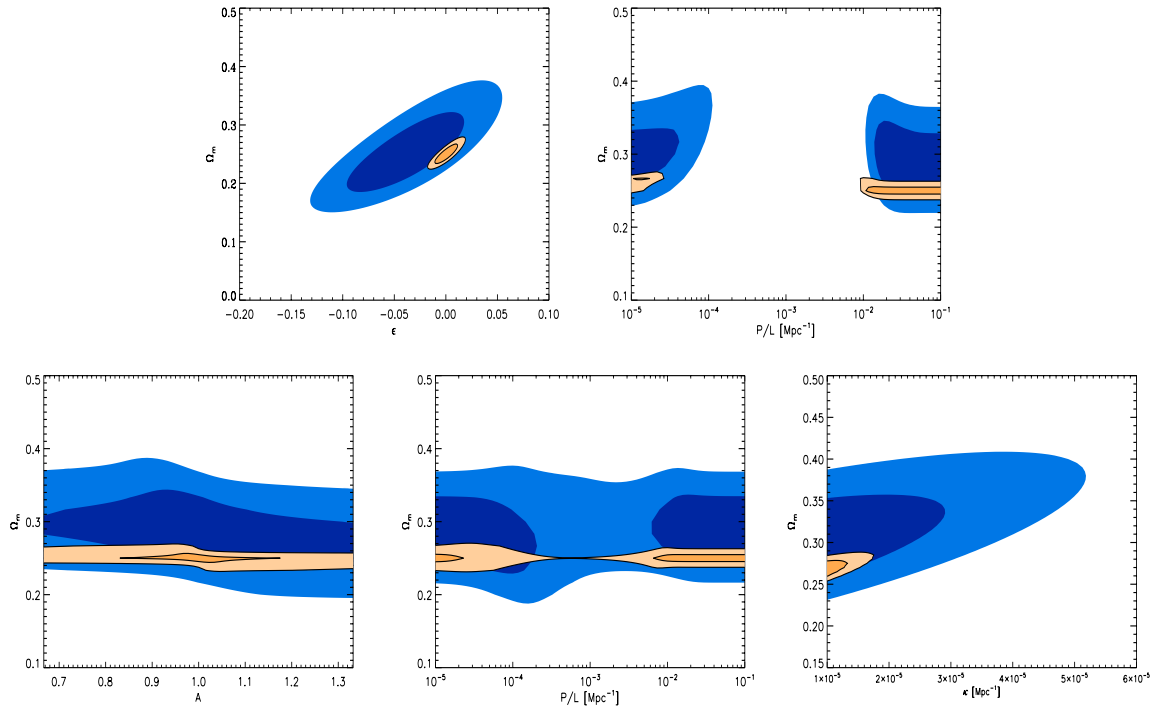


**Figure IX.** Forecast constraints from joint EUCLID (orange scale), shown together with the corresponding constraints from current data, namely SN (Union08) joint with chronometer  $H(z)$  (blue scale). Dark and light contours correspond to 1- and 2- $\sigma$  respectively. From top left to bottom right: constraints on the opacity parameter  $\epsilon$ , parameter  $P/L$  for the simple ALP model of section, parameters  $A$  &  $P/L$  for chameleons, and parameter  $\kappa$  for MCPs see Ref. [106] for more details.

into photons, resulting in a redshift-independent dimming of supernovae which we cannot constrain or exclude with cosmic opacity bounds.

The improved measurement of the cosmic opacity found here leads to improved bounds on these exotic physics scenarios which are summarised in Fig. IX. Future measurements of baryon acoustic oscillations, and an increase in the number of observations of high redshift supernovae will lead to further improvements in the constraints on physics beyond the standard model.

## References

- [1] S. Perlmutter *et al.* [Supernova Cosmology Project Collaboration], *Astrophys. J.* **517** (1999) 565 [arXiv:astro-ph/9812133]; A. G. Riess *et al.* [Supernova Search Team Collaboration], *Astron. J.* **116** (1998) 1009 [arXiv:astro-ph/9805201].
- [2] G. Jungman, M. Kamionkowski, A. Kosowsky and D. N. Spergel, *Phys. Rev. D* **54** (1996) 1332 [arXiv:astro-ph/9512139]; G. Jungman, M. Kamionkowski, A. Kosowsky and D. N. Spergel, *Phys. Rev. Lett.* **76**

- (1996) 1007 [arXiv:astro-ph/9507080]; P. de Bernardis *et al.* [Boomerang Collaboration], *Nature* **404** (2000) 955 [arXiv:astro-ph/0004404]; A. D. Miller *et al.*, *Astrophys. J.* **524** (1999) L1 [arXiv:astro-ph/9906421]; S. Hanany *et al.*, *Astrophys. J.* **545** (2000) L5 [arXiv:astro-ph/0005123]; A. H. Jaffe *et al.* [Boomerang Collaboration], *Phys. Rev. Lett.* **86** (2001) 3475 [arXiv:astro-ph/0007333]; N. W. Halverson *et al.*, *Astrophys. J.* **568** (2002) 38 [arXiv:astro-ph/0104489]; B. S. Mason *et al.*, *Astrophys. J.* **591** (2003) 540 [arXiv:astro-ph/0205384]; A. Benoit *et al.* [the Archeops Collaboration], *Astron. Astrophys.* **399** (2003) L25 [arXiv:astro-ph/0210306]; J. H. Goldstein *et al.*, *Astrophys. J.* **599** (2003) 773 [arXiv:astro-ph/0212517]; D. N. Spergel *et al.* [WMAP Collaboration], *Astrophys. J. Suppl.* **148** (2003) 175 [arXiv:astro-ph/0302209]; C. L. Reichardt *et al.*, *Astrophys. J.* **694** (2009) 1200 [arXiv:0801.1491 [astro-ph]]; C. L. Reichardt *et al.*, arXiv:0801.1491 [astro-ph]; D. N. Spergel *et al.* [WMAP Collaboration], *Astrophys. J. Suppl.* **170** (2007) 377 [arXiv:astro-ph/0603449]; J. Dunkley *et al.* [WMAP Collaboration], *Astrophys. J. Suppl.* **180** (2009) 306 [arXiv:0803.0586 [astro-ph]].
- [3] W. J. Percival *et al.* [The 2dFGRS Collaboration], *MNRAS* **327** (2001) 1297 [arXiv:astro-ph/0105252].
- [4] S. Dodelson *et al.* [SDSS Collaboration], *Astrophys. J.* **572** (2001) 140 [arXiv:astro-ph/0107421].
- [5] W. L. Freedman *et al.* [HST Collaboration], *Astrophys. J.* **553** (2001) 47 [arXiv:astro-ph/0012376].
- [6] P. J. E. Peebles and B. Ratra, *Rev. Mod. Phys.* **75**, 559 (2003) [arXiv:astro-ph/0207347]; T. Padmanabhan, *Phys. Rept.* **380** (2003) 235 [arXiv:hep-th/0212290]; E. J. Copeland, M. Sami and S. Tsujikawa, *Int. J. Mod. Phys. D* **15** (2006) 1753 [arXiv:hep-th/0603057]; J. Frieman, M. Turner and D. Huterer, *Ann. Rev. Astron. Astrophys.* **46** (2008) 385 [arXiv:0803.0982 [astro-ph]]; E. V. Linder, *Rept. Prog. Phys.* **71** (2008) 056901 [arXiv:0801.2968 [astro-ph]]; R. R. Caldwell and M. Kamionkowski, arXiv:0903.0866 [astro-ph.CO];
- [7] B. Ratra and P. J. E. Peebles, *Phys. Rev. D* **37** (1988) 3406; R. R. Caldwell, R. Dave and P. J. Steinhardt, *Phys. Rev. Lett.* **80**, 1582 (1998) [arXiv:astro-ph/9708069].
- [8] J. A. Peacock, P. Schneider, G. Efstathiou, J. R. Ellis, B. Leibundgut, S. J. Lilly and Y. Mellier, arXiv:astro-ph/0610906.
- [9] D. Stern, R. Jimenez, L. Verde, S. A. Stanford and M. Kamionkowski, *Astrophys. J. Suppl.*, **188**, (2010) 280
- [10] A. Albrecht *et al.*, arXiv:astro-ph/0609591;
- [11] W. J. Percival, S. Cole, D. J. Eisenstein, R. C. Nichol, J. A. Peacock, A. C. Pope and A. S. Szalay, *MNRAS* **381** (2007) 1053 [arXiv:0705.3323 [astro-ph]].
- [12] D. J. Eisenstein *et al.* [SDSS Collaboration], *Astrophys. J.* **633** (2005) 560 [arXiv:astro-ph/0501171].
- [13] J. B. Oke *et al.*, *Publ. Astrophys. Soc. Pac.* **107** (1995) 375
- [14] H. J. Seo and D. J. Eisenstein, *Astrophys. J.* **598** (2003) 720 [arXiv:astro-ph/0307460].
- [15] J. R. Pritchard, S. R. Furlanetto and M. Kamionkowski, *MNRAS* **374** (2007) 159 [arXiv:astro-ph/0604358].
- [16] Z. Haiman, J. J. Mohr and G. P. Holder, *Astrophys. J.* **553** (2000) 545 [arXiv:astro-ph/0002336].
- [17] A. Refregier, *Ann. Rev. Astron. Astrophys.* **41** (2003) 645 [arXiv:astro-ph/0307212].

- [18] R. Jimenez and A. Loeb, *Astrophys. J.* **573** (2002) 37 [arXiv:astro-ph/0106145].
- [19] B. Chaboyer, *Astrophys. J.* **444** (1995) L9 [arXiv:astro-ph/9412015].
- [20] R. Jimenez, U. G. Jorgensen, P. Thejll and J. MacDonald, *MNRAS* **275** (1995) 1245 [arXiv:astro-ph/9502050].
- [21] L. M. Krauss and B. Chaboyer, *Science* **299** (2003) 65.
- [22] R. Jimenez, L. Verde, T. Treu and D. Stern, *Astrophys. J.* **593**, 622 (2003) [arXiv:astro-ph/0302560].
- [23] J. Simon, L. Verde and R. Jimenez, *Phys. Rev. D* **71** (2005) 123001 [arXiv:astro-ph/0412269].
- [24] M. Sahlen, A. R. Liddle and D. Parkinson, *Phys. Rev. D* **72** (2005) 083511 [arXiv:astro-ph/0506696]; L. Samushia and B. Ratra, *Astrophys. J.* **650** (2006) L5 [arXiv:astro-ph/0607301]; R. Lazkoz, *AIP Conf. Proc.* **960** (2007) 3 [arXiv:0710.2872 [astro-ph]]; N. E. Mavromatos and V. A. Mitsou, *Astropart. Phys.* **29** (2008) 442 [arXiv:0707.4671 [astro-ph]]; F. C. Carvalho, E. M. Santos, J. S. Alcaniz and J. Santos, *JCAP* **0809** (2008) 008 [arXiv:0804.2878 [astro-ph]]; E. Fernandez-Martinez and L. Verde, *JCAP* **0808** (2008) 023 [arXiv:0806.1871 [astro-ph]]; A. Kurek, O. Hrycyna and M. Szydlowski, *Phys. Lett. B* **659** (2008) 14 [arXiv:0707.0292 [astro-ph]]; A. A. Sen and R. J. Scherrer, *Phys. Lett. B* **659** (2008) 457 [arXiv:astro-ph/0703416]; H. Zhang and Z. H. Zhu, *JCAP* **0803** (2008) 007 [arXiv:astro-ph/0703245]; B. Ratra and M. S. Vogeley, *Publ. Astron. Soc. Pac.* **120** (2008) 235 [arXiv:0706.1565 [astro-ph]];
- [25] J. Dunlop, J. Peacock, H. Spinrad, A. Dey, R. Jimenez, D. Stern and R. Windhorst, *Nature* **381** (1996) 581.
- [26] H. Spinrad, A. Dey, D. Stern, J. Dunlop, J. Peacock, R. Jimenez and R. Windhorst, *Astrophys. J.* **484** (1997) 581. arXiv:astro-ph/9702233.
- [27] L. L. Cowie, A. Songaila and A. J. Barger, Density for  $z < 1$ ," *Astron. J.* **118** (1999) 603 [arXiv:astro-ph/9904345].
- [28] A. Heavens, B. Panter, R. Jimenez and J. Dunlop, *Nature* **428** (2004) 625 [arXiv:astro-ph/0403293].
- [29] D. Thomas, C. Maraston, R. Bender and C. M. de Oliveira, *Astrophys. J.* **621** (2005) 673 [arXiv:astro-ph/0410209].
- [30] B. Panter, R. Jimenez, A. F. Heavens and S. Charlot, *MNRAS* **378** (2007) 1550 [arXiv:astro-ph/0608531].
- [31] T. Treu *et al.*, *Astrophys. J.* **633**, 174 (2005) [arXiv:astro-ph/0503164].
- [32] Stern, D., Jimenez, R., Verde, L., Kamionkowski, M., Stanford, S. A. 2010. *JCAP* 2, 8.
- [33] Moresco M., Jimenez R., Cimatti A., Pozzetti L., 2011, *JCAP*, 3, 45
- [34] Moresco M., et al., 2012, *JCAP*, 8, 6
- [35] Moresco M., Verde L., Pozzetti L., Jimenez R., Cimatti A., 2012, *JCAP*, 7, 53
- [36] Jimenez R., Talavera P., Verde L., Moresco M., Cimatti A., Pozzetti L., 2012, *JCAP*, 3, 14
- [37] Moresco M., Jimenez R., Cimatti A., Pozzetti L., 2011, *JCAP*, 3, 45
- [38] Bellini E., Jimenez R., 2013, arXiv, arXiv:1306.1262
- [39] de Putter R., Verde L., Jimenez R., 2013, *JCAP*, 2, 47
- [40] Hoyle B., Tojeiro R., Jimenez R., Heavens A., Clarkson C., Maartens R., 2013, *ApJ*, 762, L9

- [41] Heavens A. F., Jimenez R., Maartens R., 2011, JCAP, 9, 35
- [42] Verde L., Jimenez R., Feeney S., 2013, arXiv, arXiv:1303.5341
- [43] Verde L., Protopapas P., Jimenez R., 2013, arXiv, arXiv:1306.6766
- [44] Y. Fukuda *et al.*, Phys. Rev. Lett. **81**, 1562 (1998).
- [45] Ahn, M. H., *et al.*, Phys. Rev. D **74**, 072003 (2006).
- [46] Adamson P., *et al.*, Phys. Rev. Lett. **101**, 221804 (2008)
- [47] Q. R. Ahmad *et al.*, Phys. Rev. Lett. **89**, 011301 (2002).
- [48] K. Eguchi *et al.*, Phys. Rev. Lett. **90**, 021802 (2003).
- [49] B. T. Cleveland *et al.*, Astrophys. J. **496**, 505 (1998).
- [50] E. Bellotti, Talk at VIIIth International Conference on Topics in Astroparticle and Underground Physics (TAUP03), Seattle, (Sep 5-9, 2003); V. Gavrin, *ibid.*
- [51] J. N. Bahcall, Phys. Rev. Lett. **12**, 300 (1964); R. Davis, Phys. Rev. Lett. **12**, 303 (1964).
- [52] L. Wolfenstein, Phys. Rev. D **17**, 2369 (1978); S. P. Mikheev and A. Y. Smirnov, Sov. J. Nucl. Phys. **42**, 913 (1985).
- [53] H. Murayama and C. Pena-Garay, Phys. Rev. D **69**, 031301 (2004).
- [54] Melchiorri, A., Mena, O., Palomares-Ruiz, S., Pascoli, S., Slosar, A., & Sorel, M., JCAP, 1, 36 (2009)
- [55] A. A. Aguilar-Arevalo *et al.*, Phys. Rev. Lett. **98**, 231801 (2007).
- [56] M. Fukugita and T. Yanagida, Phys. Lett. B **174**, 45 (1986).
- [57] Cremonesi, O. 2010, arXiv:1002.1437
- [58] E. Komatsu *et al.*, Astrophys. J. Suppl. **180** (2009) 330.
- [59] Reid, B. A., Verde, L., Jimenez, R., & Mena, O. 2010, JCAP, 1, 3
- [60] LSST Science Collaborations: Paul A. Abell, *et al.* 2009, arXiv:0912.0201
- [61] Hannestad, S. 2010, arXiv:1003.4119
- [62] Refregier, A., Amara, A., Kitching, T. D., Rassat, A., Scaramella, R., Weller, J., & Euclid Imaging Consortium, *et al.* 2010, arXiv:1001.0061
- [63] Slosar, A. 2006, Phys. Rev. D., **73**, 123501
- [64] Jimenez, R., Kitching, T., Peña-Garay, C., Verde, L. 2010. JCAP 5, 35.
- [65] M. Takada, E. Komatsu and T. Futamase, Phys. Rev. D **73**, 083520 (2006).
- [66] de Bernardis, F., Kitching, T. D., Heavens, A., & Melchiorri, A. 2009, PRD, **80**, 123509
- [67] D. J. Eisenstein and W. Hu, Astrophys. J. **511** (1997) 5.
- [68] Fisher, R. A. 1932, Proceedings of the Cambridge Philosophical Society, **28**, 257
- [69] Heavens, A. F., Kitching, T. D., & Verde, L. 2007, MNRAS, **380**, 1029
- [70] Taylor, A. N., & Kitching, T. D. 2010, arXiv:1003.1136
- [71] H. J. Seo and D. J. Eisenstein, Astrophys. J. **598**, 720 (2003).
- [72] Wagner C., Verde L., Jimenez R., 2012, ApJ, **752**, L31

- [73] Etherington, J. M. H. 1933, *Phil. Mag.*, 15, 761
- [74] Ménard, B. et al. 2008, *MNRAS*, 385, 1053
- [75] Bovy, J., Hogg, D. W., & Moustakas, J. 2008, *ApJ*, 688, 198
- [76] Aguirre, A. N. 1999, *ApJL*, 512, L19
- [77] Jaeckel, J., & Ringwald, A., arXiv:1002.0329 [hep-ph]
- [78] Csáki, C., Kaloper, N., & Terning, J., *Phys. Rev. Lett.* **88** (2002) 161302
- [79] Mörtzell, E., Bergström, L., & Goobar, A., *Phys. Rev. D* **66** (2002) 047702
- [80] Mirizzi, A., Raffelt, G. G., & Serpico, P. D., *Lect. Notes Phys.* **741**, 115 (2008) [arXiv:astro-ph/0607415]
- [81] Burrage, C., *Phys. Rev. D* **77** (2008) 043009 [arXiv:0711.2966 [astro-ph]]
- [82] Ahlers, M., *Phys. Rev. D* **80** (2009) 023513 [arXiv:0904.0998 [hep-ph]]
- [83] Kostelecky, V. A., & Russell, N. 2008, arXiv:0801.0287 [hep-ph]
- [84] Bassett B. A., & Kunz, M., *Astrophys. J.* **607**, 661 (2004)
- [85] Bassett B. A., & Kunz, M., *Phys. Rev. D* **69**, 101305 (2004)
- [86] Uzan, J. P. *Gen. Rel. Grav.* **39** (2007) 307 [arXiv:astro-ph/0605313]
- [87] Lazkoz, R., Nesseris, S. & Perivolaropoulos, L. 2008, *JCAP* **0807** 012 [arXiv:0712.1232 [astro-ph]]
- [88] Percival, W. J. et al. 2007, *MNRAS*, 381, 1053
- [89] Riess, A.G., *et al.*, *Astrophys. J.* **699** (2009) 539 [arXiv:0905.0695 [astro-ph.CO]]
- [90] Freedman, W. L., *et al.* 2001, *ApJ*, 553, 47
- [91] Song, Y. S., & Hu, W., *Phys. Rev. D* **73** (2006) 023003 [arXiv:astro-ph/0508002]
- [92] More, S., Bovy, J., & Hogg, D. W. 2008, arXiv:0810.5553
- [93] Avgoustidis, A., Verde, L., & Jimenez, R., *JCAP* **0906** (2009) 012 [arXiv:0902.2006 [astro-ph.CO]]
- [94] Kowalski *et al.* 2008, *ApJ*, 686, 749
- [95] Jimenez, R., Verde, L., Treu, T., & Stern, D., 2003, *ApJ*, 593, 622
- [96] Peccei, R. D., & Quinn, H. R., *Phys. Rev. Lett.* **38** (1977) 1440.
- [97] Svrcek, P., & Witten, E., *JHEP* **0606** (2006) 051 [arXiv:hep-th/0605206]
- [98] Anselm, A. A., & Uraltsev, N. G., *Phys. Lett.* **B114** (1982) 39-41.
- [99] Brax, P., Burrage, C., Davis, A. C., Seery, D., & Weltman, A., arXiv:0911.1267 [hep-ph]
- [100] Khoury, J., & Weltman, A., *Phys. Rev. Lett.* **93** (2004) 171104 [arXiv:astro-ph/0309300]
- [101] Khoury, J., & Weltman, A., *Phys. Rev. D* **69** (2004) 044026 [arXiv:astro-ph/0309411]
- [102] Burrage, C., Davis, A. C., & Shaw, D. J., *Phys. Rev. D* **79** (2009) 044028 [arXiv:0809.1763 [astro-ph]]
- [103] Brax, P., van de Bruck, C., Davis, A. C., Khoury, J., & Weltman, A., *Phys. Rev. D* **70** (2004) 123518 [arXiv:astro-ph/0408415]
- [104] Brax, P., van de Bruck, C., & Davis, A. C., *Phys. Rev. Lett.* **99** (2007) 121103 [arXiv:hep-ph/0703243]
- [105] Raffelt, G., & Stodolsky, L., *Phys. Rev. D* **37** (1988) 1237.
- [106] Avgoustidis, A., Burrage, C., Redondo, J., Verde, L., Jimenez, R. 2010. *JCAP* 10, 24.